

Melt Crystallization of Bisphenol A Polycarbonate in Blends of Polycarbonate with Zinc Salts of Sulfonated Polystyrene Ionomers

Liang Xu[‡] and R. A. Weiss^{*,†,‡}

Department of Chemical Engineering and Polymer Program, University of Connecticut, Storrs, Connecticut 06269-3136

Received July 22, 2003; Revised Manuscript Received September 17, 2003

ABSTRACT: The addition of zinc salts of sulfonated polystyrene ionomers (ZnSPS) to bisphenol A polycarbonate (PC) induced melt crystallization of the PC. This phenomenon was investigated using differential scanning calorimetry and wide-angle X-ray diffraction. Gel permeation chromatography was used to monitor changes in molecular weight to assess whether polymer degradation was responsible for the melt crystallization. Fourier transform infrared spectroscopy and small-angle X-ray scattering were used to evaluate specific interaction and the microstructure of the blends. Melt crystallization of PC at 190 °C was accelerated in both single-phase and phase-separated blends. The crystallization induction time ranged from 1 to 42 h depending on the sulfonation level of the ionomer, and crystallinities of 20%–28% were achieved. An Avrami analysis of the crystallization kinetics indicated that the crystallization was a nucleated process. Although some molecular weight reduction of the PC did occur during thermal annealing at elevated temperatures, it was not considered responsible for the crystallization. Unlike previous work where melt crystallization of PC was induced by a “chemical nucleation” with alkali salts of aromatic carboxylic acids, crystallization in the PC–ZnSPS blends was reversible. Although the origin of the crystallization was not determined, it appeared that the nanometer-sized ionic aggregates associated with the ionomer, which were present even in the single-phase blends, contributed to the crystal nucleation.

Introduction

The poly(aryl carbonate) derived from 2,2-bis(4-hydroxyphenyl)propane, commonly known as bisphenol A polycarbonate (PC), is usually a clear, amorphous plastic when processed from the melt state.¹ It is, nonetheless, a crystallizable polymer, but because of the rigidity of the PC chain, its melt crystallization kinetics is extremely slow. Exceedingly long times are needed (> 100 h) to complete the crystallization, and a crystallinity of about 20% can be obtained by melt crystallization.² Crystalline PC can also be produced by either precipitating the polymer from solution or by exposing the polymer to solvent vapors.³ Solvents reported to promote crystallization of PC include acetone, ethyl acetate, and tetrachloroethylene.⁴ Solvent-induced crystallization of PC proceeds rapidly, within several minutes or hours, compared to melt crystallization, and the crystallinity achieved can be as high as 24%, depending on the solvent used.⁴ Supercritical carbon dioxide⁵ and plasticizers such as trimellitic acid tridecylolyl (TATE)⁶ also facilitate crystallization of PC.

Legras and co-workers^{7–13} reported that the melt crystallization rate of PC increased significantly in the presence of 0.1–1 wt % sodium *o*-chlorobenzoate (SOCB) or sodium *o*-chlorophenolate (SOCP). Crystallization at 220 °C was completed within 1 h, and crystallinity as high as 50% was achieved. However, after melting, the PC did not crystallize again. The enhanced crystallization rate was attributed to nucleophilic attack of SOCB on the carbonate group,^{8–11} which also severely degraded the PC molecular weight and reduced the melt viscosity. The authors called the nucleation of PC by SOCB and SOCP “chemical nucleation” to distinguish

it from conventional heterogeneous nucleation where no chemical reaction occurs.^{7–13}

Lightly sulfonated polystyrene ionomers (SPS) are miscible with PC for a range of sulfonation level that depends on the cation used, and the blends exhibit upper critical solution temperature (UCST) phase behavior.^{14–16} Weiss and co-workers^{16,17} reported that the PC in PC/SPS blends crystallized when the blend was cooled from the melt, but the phenomenon was not well characterized in those papers. This paper provides a more complete description of the effect of SPS on the crystallization of PC.

Experimental Details

Materials. PC (Lexan OQ1050C) with $M_w = 31\,000$ g/mol and $M_w/M_n = 1.90$ was provided by General Electric Corp. and was used as received. Polystyrene (PS) with $M_n = 4000$ g/mol and $M_w/M_n = 1.06$ was obtained from Pressure Chemical Co. Sulfonated polystyrene ionomers (SPS) were prepared by sulfonating the PS in a 1,2-dichloroethane solution with acetyl sulfate at 50 °C following the procedure of Makowski et al.¹⁸ The sulfonation reaction is an electrophilic substitution reaction, which substitutes a sulfonic acid group primarily at the para position of the phenyl ring; the sulfonation is random along the chain. The sulfonation level was determined by titration of the sulfonic acid derivative, HSPS, in a mixed solvent of toluene/methanol (90/10 v/v) with methanolic sodium hydroxide. Zinc salts (ZnSPS) were prepared by neutralizing the HSPS in a toluene/methanol solution with a 20% excess of zinc acetate dissolved in methanol. The ionomers were isolated from solution by steam stripping, filtered, washed several times with deionized water, and dried under vacuum. The ionomer was then extracted with methanol using a Soxhlet extractor for 1 week to remove all excess zinc acetate and then dried at 150 °C under vacuum. The ionomer nomenclature used in this paper is ZnSPS_{x,y}, where *x,y* is the sulfonation level, i.e., the mole percent of styrene repeat units that were sulfonated. The characteristics of the ionomers and the PC are summarized in Table 1.

[†] Department of Chemical Engineering.

[‡] Polymer Program.

* Corresponding author.

Table 1. Characteristics of Pure Components

material	M_w (g mol ⁻¹)	M_w/M_n	T_g (°C)
PC	31000	1.90	146
PS	4000	1.04	78
ZnSPS3.8	4000	1.04	85
ZnSPS7.4	4000	1.04	94
ZnSPS10.0	4000	1.04	99
ZnSPS11.3	4000	1.04	103
ZnSPS12.7	4000	1.04	107

Sodium tosylate (NaTS), $C_7H_7SO_3Na$, was obtained from ACROS Chemical Co. Zinc tosylate (ZnTS), $C_{14}H_{14}S_2O_6Zn$, was synthesized by neutralizing an aqueous solution of *p*-toluene-sulfonic acid (Aldrich Chemical Co.) with a stoichiometric amount of the zinc acetate dihydrate (ACROS Chemical Co.). The ZnTS was dried at ca. 30 °C in air for several days, at 150 °C under vacuum for 1 day, and finally at 250 °C under vacuum for 1 h. Sodium benzoate, $C_6H_5O_2Na$, was obtained from Aldrich Chemical Co.

PC–ZnSPS blends were prepared by adding a 2% (w/v) PC solution in tetrahydrofuran (THF) dropwise to a stirred 2% (w/v) solution of ZnSPS in THF. The PC/THF and ZnSPS/THF solutions were filtered with a microfilter with a pore size of 1 μ m before mixing. The mixture solution was then poured into a poly(tetrafluoroethylene) dish covered with perforated aluminum foil, which allowed the solvent to slowly evaporate. The cast blend films were dried in a vacuum oven at room temperature for 2 days, at 60 °C for 3 days, at 100 °C for 2 days, and finally at 170 °C for 1 h. The dried films were sealed in 4 mL glass vials equipped with screw caps and stored in a desiccator prior to the crystallization experiments. The blend nomenclature used in this paper is PC–ZnSPS $x.y$ (n/m), where (n/m) denotes the PC/ZnSPS composition (w/w).

Model mixtures of PC with 2% NaTS (PC–NaTS(98/2)) and 1% ZnTS (PC–ZnTS(99/1)) were prepared by melt mixing at 250 °C for 7 min in a Brabender Plasticorder; a similar procedure was used by Legras et al.⁷ for the preparation of PC/SOCB and PC/SOCP mixtures. The tosylate concentrations used corresponded to molar concentrations of sulfonate groups similar to what was present in the PC–ZnSPS blends.

Polymer Characterization. Thermal transitions were measured with a Perkin-Elmer differential scanning calorimeter, DSC-7. The DSC was calibrated with indium and tin standards. The samples varied from 5 to 15 mg and were crimped into aluminum pans inside a glovebox with a dry nitrogen atmosphere.

Melt crystallization of the PC in the blend and the miscibility of the blend were assessed by first heating a film in the DSC to 250 °C, annealing it at 250 °C for 10 min to eliminate the prior thermal and solvent history, quenching it to 190 °C, and finally annealing it at 190 °C for 0–48 h. The annealed specimen was then quenched quickly in the DSC to 30 °C, nominally at 80 °C/min, followed by a DSC heating experiment at 20 °C/min to measure the enthalpy of fusion (ΔH_f) and the glass transition temperature(s) (T_g). ΔH_f was calculated from the integrated area under the melting endotherm; the enthalpy was calibrated using indium and zinc standards. T_g was defined as the midpoint of the change in the heat capacity at the transition. The cooling rate used in the quenching step following annealing was assumed to be fast enough so that the subsequent heating thermogram represented the morphology of the blend at the annealing temperature.

Fourier transform infrared (FTIR) spectra were measured with a Nicolet 560 Magna-IR spectrometer. Samples for FTIR analysis were obtained by removing the crystallized blend from the DSC pan following a DSC experiment, grinding it to powder, mixing it with KBr powder, and then pressing the mull into a film. The sample was then dried in a vacuum oven at 100 °C for 1 day. A total of 128 scans were signal averaged for each spectrum, and the resolution was 1 cm⁻¹.

Molecular weight distributions were measured by gel permeation chromatography (GPC) using a Waters 150-C GPC equipped with a Waters 2487 dual λ -absorbance detector; the detector was set to measure the absorbance at 254 nm. Four

microstyragel columns with pore sizes of 10⁴, 10³, 50, and 10 nm were used. The combination of these four columns provided measurement of molecular weights from 10² to 4 \times 10⁶ g/mol. A universal calibration procedure using PS standards was employed. The mobile phase was THF, and the flow rate was set at 1 mL/min. Samples for the GPC measurements were obtained from the DSC specimens, which were dissolved in THF to form 0.1% (w/v) solutions. The blend solutions were filtered with a 0.45 μ m microfilter before injection into the column. Solutions of the neat PC and ZnSPS with the same concentrations used for the blend solutions were also measured, and the molecular weight of the PC in the blend solution was calculated by subtracting the pure ZnSPS signal from the blend solution curve.

Wide-angle X-ray diffraction (WAXD) was performed on a Bruker D8 Advance wide-angle X-ray diffractometer using Cu K α (λ = 0.154 nm) radiation. The samples for the X-ray study were crystallized in the DSC and then transferred to the WAXD sample holder. A scanning rate of 1°/min over a range of scattering angles, 2θ = 5–35°, was used.

Small-angle X-ray scattering (SAXS) was measured with a Bruker SAXS instrument equipped with a Ni filter, pinhole collimation, and a Histar area detector. Cu K α radiation was obtained from a Rigaku rotating anode operating at 40 kV and 100 mA. The sample-to-detector distance was fixed at 108 cm, yielding a wavevector, q , range of 0.18–3.25 nm⁻¹, where $q = 4\pi \sin \theta/\lambda$, where 2θ is the scattering angle. Bragg's law, $d = 2\pi/q$, was used to relate the scattering wavevector and the size of the scattering object in real space. The background scattering was determined by running SAXS on the empty sample chamber, and this was subtracted from the SAXS of the sample.

A Nikon polarizing optical microscope was used to view the PC crystal morphology. The microscopy specimens were prepared by casting a thin polymer film THF onto a glass coverslip, which was dried under vacuum at 170 °C. The sample was then transferred to a heating plate in a glovebox purged with dry nitrogen. The sample was pressed into a 10–20 μ m film between two cover glasses above at ca. 250 °C using a metal plate on top of the upper cover glass to provide a uniform force on the sample. The 250 °C heat treatment was above the melting point of PC in the blend (ca. 230 °C), which was sufficient to erase the previous solvent and thermal history of the specimen. The melt was quenched to room temperature, and the sample was sealed in a glass container purged with nitrogen and then stored in the desiccator. For microscopy measurements, the sample was transferred directly from the desiccator to a hot stage preheated to 190 °C and with a nitrogen purge. The sample was then annealed for a specified crystallization time before the morphology was observed.

Results and Discussion

Phase Behavior of PC/ZnSPS Blends. Xie and Weiss^{14,15} and Lu and Weiss¹⁶ previously studied the phase behavior of PC/SPS blends using a variety of experimental techniques, including thermal analysis, optical microscopy, light scattering, and FTIR spectroscopy. SPS ionomers with a variety of counterions, e.g., Na⁺, Li⁺, Zn²⁺, are miscible with PC over some range of sulfonation level that depends on the particular cation used. Miscibility was attributed to the strong unfavorable intramolecular interaction between the sulfonated styrene and the neutral styrene repeat units in the ionomer, i.e., a copolymer effect.^{19–21} The blends exhibited upper critical solution temperature (UCST) phase behavior.^{14–16} Depending on the sulfonation level of the ionomer and the blend composition, the UCST for PC–ZnSPS blends ranged from 170 to 300 °C. The miscibility of PC–ZnSPS blend can be enhanced by either decreasing the molecular weight of either or both components in the blend or increasing the sulfonation

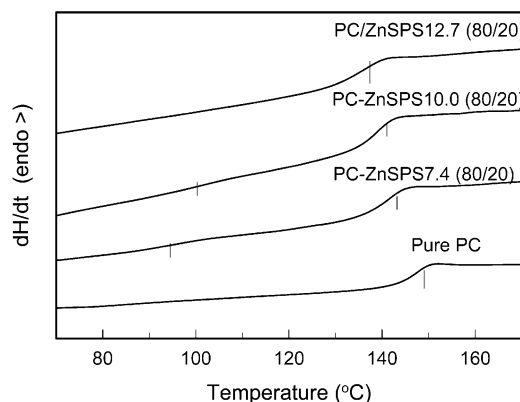


Figure 1. DSC heating thermograms of PC-ZnSPS x, y (80/20) blends annealed at 190 °C. The marks on the curves denote T_g 's.

level of the ZnSPS.^{14–16} A low molecular weight PS (4000 Da) was chosen for this research to provide a relatively low UCST. Previous studies^{15,16} showed that crystallization of PC also occurred in blends with higher molecular weight ($\sim 100\,000$ Da) SPS ionomers, so the results described in this paper are not believed to be unique for the low molecular weight ionomers.

For the present study, the phase behavior of PC-ZnSPS at 190 °C was particularly important because the crystallization studies were carried out at that temperature. PC crystallizes fastest at 190 °C.^{22,23} Representative DSC heating thermograms of three different PC-ZnSPS blends after annealing for 1 h at 190 °C are shown in Figure 1. It was assumed that the samples were quenched fast enough to room temperature, which is below the T_g of both components, so that the subsequent heating thermogram represents the state of the blend at the annealing temperature. All of the blends had the same composition (80/20 w/w PC/ZnSPS), but the sulfonation level of the ionomer used varied from 7 to 13 mol %. When the sulfonation level of the ZnSPS was below 10%, the thermogram exhibited two T_g 's, which indicates a two-phase morphology at 190 °C. However, the higher T_g in those blends was lower than that of the neat PC, and it shifted to lower temperature with increasing sulfonation level, which indicates partial miscibility of the PC and the ionomer at 190 °C. The lower T_g shifted to higher temperature with increasing sulfonation level, but it coincided with that of the pure ionomer with the same sulfonation level (the T_g of the ionomer also increased with increasing sulfonation level, see Table 1), which indicates that the dispersed phase was pure ionomer. The thermogram for the blend with the highest sulfonated ionomer, 12.7 mol %, showed only a single T_g , which was between the T_g of the two components, which indicates a single-phase, miscible blend.

Figure 2 shows a liquid-liquid miscibility map, determined from DSC analyses similar to that described for Figure 1, i.e., for PC-ZnSPS blends annealed for 1 h at 190 °C. The open circles represent DSC scans exhibiting one T_g , i.e., a single-phase blend, and the filled circles represent DSC scans exhibiting two T_g 's, or two-phase blends. For a fixed composition, the miscibility improved with increasing sulfonation level, and for a fixed sulfonation level, miscibility increased as the ionomer content in the blend decreased. Those observations are in agreement with our previous studies of the phase behavior of PC-ZnSPS blends, which used

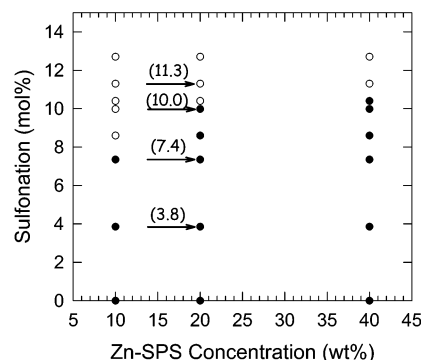


Figure 2. Miscibility map for PC-ZnSPS blends at 190 °C. The filled circles denote immiscible blends; the open circles denote miscible blends. The numbers and arrows in the figure indicate the sulfonation levels and blend composition of the samples used in the crystallization experiments (see text).

different molecular weight polymers.^{14,15} A miscibility map was also constructed for samples annealed at 250 °C and was nearly identical to that shown in Figure 2, which indicates that a cloud point was not encountered when samples were heated to 250 °C prior to the crystallization experiments that are described below.

Figure 2 indicates that, of the four blends whose crystallization behavior was evaluated (marked by arrows in Figure 2), the PC-ZnSPS11.3 (80/20) was a miscible, single-phase blend at 190 °C, while PC-ZnSPS3.8 (80/20), PC-ZnSPS7.4 (80/20) and PC-ZnSPS10.0 (80/20) were two-phase blends. The temperatures of the two T_g 's for the latter three blends (see Figure 1) indicated that a pure ionomer phase was dispersed in a PC continuous phase that contained some ionomer and that the ZnSPS content of the PC-rich phase increased with increasing sulfonation level of the ionomer. The composition of all four blends discussed in this paper was fixed at 80 wt % PC, so hereforth in this paper the (80/20) nomenclature is dropped from the sample designation. For that composition, the sulfonation levels used in this study, ca. 4–13 mol %, correspond to about 0.1–0.2 wt % zinc sulfonate, which is comparable to the 0.1–1 wt % SOCB and SOCP (see Introduction) used by Legras and co-workers^{7–13} in their work on chemical nucleation of PC.

Crystallization Kinetics. Representative DSC thermograms obtained after annealing PC-ZnSPS11.3 for various times at 190 °C are shown in Figure 3. Crystallization of the PC occurred within a 10 h annealing time, as demonstrated by the melting endotherm near 230 °C in the DSC thermograms. The enthalpy of fusion, i.e., the area under the endotherm, increased with increasing annealing time as crystallization proceeded. Thus, it appeared that the crystallization process involved an induction period during which no crystallinity was observed, followed by a period of crystal growth. That suggests a nucleated process, as will be discussed later. For similar experiments, but with annealing at 180 or 200 °C, no crystallinity was detected after 14 h, which indicates that a maximum in the nucleation kinetics and/or the crystal growth occurred at about 190 °C. That is consistent with previous reports that the maximum crystallization rate for neat PC was at 190 °C^{22,23} and that temperature was chosen for the rest of the crystallization experiments described herein.

The melting endotherms exhibited a major peak at about 230 °C and a broad shoulder at ca. 210 °C (see Figure 3). Similar results were reported by Alizadeh and

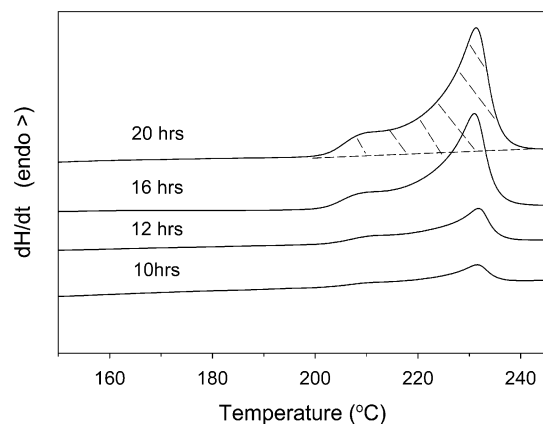


Figure 3. DSC heating thermograms of PC-ZnSPS11.3 (80/20) blends annealed at 190 °C for 10, 12, 16, and 20 h. The shaded area represents the enthalpy of fusion of the PC crystallites for the 20 h sample.

co-workers^{23,24} in studies of crystallization of neat PC and by Jonza and Porter²⁵ for supercritical CO₂-induced crystallization of PC. Alizadeh and co-workers^{23,24} attributed the small shoulder to the melting of less perfect secondary crystallites formed on the surface of the primary crystallites. In this study, the enthalpy of fusion of the PC was calculated by integrating the entire DSC endotherm, and the degree of crystallinity of the PC in the blends, X_{PC} , was calculated from eq 1

$$X_{PC} = \frac{\Delta H_f}{\Delta H_f f_{PC}} \quad (1)$$

where ΔH_f was the enthalpy of fusion calculated from the DSC endotherm, ΔH_f was the heat of fusion for 100% crystalline PC (109.7 J/g),²⁶ and f_{PC} was the mass fraction of PC in the blend.

A Hoffman and Weeks analysis²⁷ (not shown) was used to calculate the equilibrium melting point of PC, T_m° , in the three blends with the higher sulfonated ionomers. The crystallization rate for the PC-ZnSPS3.8 was too slow to obtain reliable data. T_m° decreased slightly with increasing sulfonation level: 258, 257, and 255 °C for PC-ZnSPS7.4, PC-ZnSPS10.0, and PC-ZnSPS11.3, respectively. Literature values for the melting point of PC vary widely. Nonequilibrium melting temperatures ranging from 230 to 270 °C,^{23,24,28} and equilibrium melting points of 317²⁵ and 335 °C²⁹ have been reported. The equilibrium melting points calculated in the present study are considerably lower than the extrapolated values reported in refs 25 and 29, but similar to the experimental values of T_m . The trend of decreasing T_m° with increasing sulfonation level is consistent with increasing miscibility of the ionomer in the PC phase with increasing sulfonation level and the consequential depression of the melting point.

The crystallization kinetics of the blends were determined by heating them to 250 °C for 10 min, quenching to 190 °C and annealing for a specified time, quenching the sample to room temperature, reheating it in the DSC, and calculating the degree of crystallinity as described above. The crystallization curves at 190 °C for the four blends are shown in Figure 4. For all blends, crystallization followed a long induction period during which no crystallization occurred. The 42 h induction period for PC-ZnSPS3.8 was significantly longer than for the other three samples but still substantially

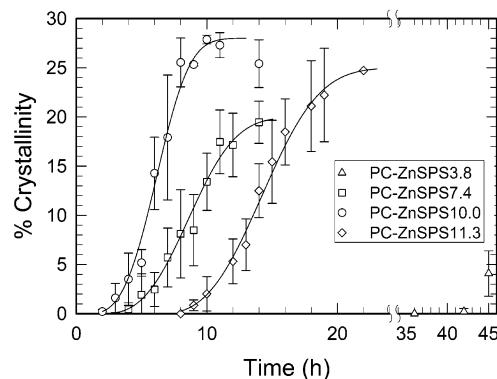


Figure 4. PC crystallinity in PC-ZnSPS *x, y* (80/20) blends as a function of annealing time at 190 °C. The solid curve represents the least-squares fit of the Avrami equation.

shorter than for neat PC.^{2,23} For the three phase-separated blends, the induction period decreased with increasing sulfonation level of the ionomer; the induction period for the PC-ZnSPS10.0 was ca. 2 h, which is 2 orders of magnitude shorter than for neat PC. When the sulfonation level was increased from 10.0 to 11.3 mol %, the blend became miscible at 190 °C, and surprisingly, the induction time increased from 2 h to ca. 8 h. For the three blends with the higher sulfonated ionomers, crystallization was complete after 6–10 h following the induction period, and the degree of crystallinity achieved was between 20 and 28%. Although the number of blends studied was limited, these data also suggest that the maximum crystallinity increased with increasing sulfonation level for the two-phase blend and then decreased again for the miscible blend. The crystallization kinetics of the neat PC were not characterized in these studies (the values reported for neat PC were taken from the literature^{2,23}), but a PC specimen subjected to the same thermal history as these blends did not crystallize when annealed at 190 °C for 16 h.

The solid curves in Figure 4 are the least squares regression of the crystallization data to the Avrami equation,³⁰

$$1 - X_t = \exp(-Kt^n) \quad (2)$$

$$X_t = X'_t/X_m \quad (3)$$

$$t = t_1 - t_0 \quad (4)$$

where K is the crystallization rate constant, n is the Avrami crystallization index, which depends on the nature of the nucleation and growth geometry of the crystals, X_t is the relative crystallinity at crystallization time t , t_0 is the induction time, X'_t is the crystallinity at time t measured by DSC, and X_m is the maximum crystallinity of the blend. In principle, X_m corresponds to the crystallinity at $t = \infty$, but for these analyses, the maximum crystallinity measured for each blend (20%, 28%, and 25% for PC-ZnSPS7.4, PC-ZnSPS910.0, and PC-ZnSPS11.3, respectively) was used for X_m . Because of the long time needed to crystallize PC-ZnSPS3.8, there was insufficient data for an Avrami analysis of that blend.

The time t in eq 2 is the crystallization time, i.e., the total annealing time at 190 °C minus the induction time ($t = t_1 - t_0$). The Avrami rate constant and Avrami index were determined from nonlinear least-squares fits of the

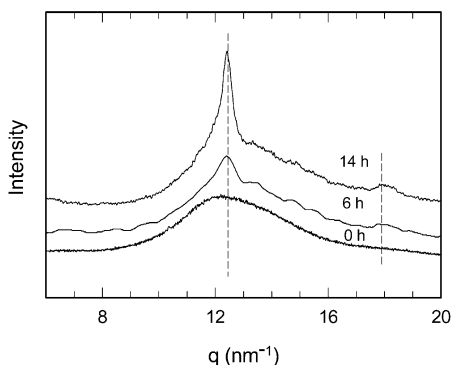


Figure 5. Time evolution of the WAXD patterns of a PC-ZnSPS10.0 (80/20) blend annealed at 190 °C. The dashed lines correspond to $q = 2.4 \text{ nm}^{-1}$ and $q = 17.9 \text{ nm}^{-1}$.

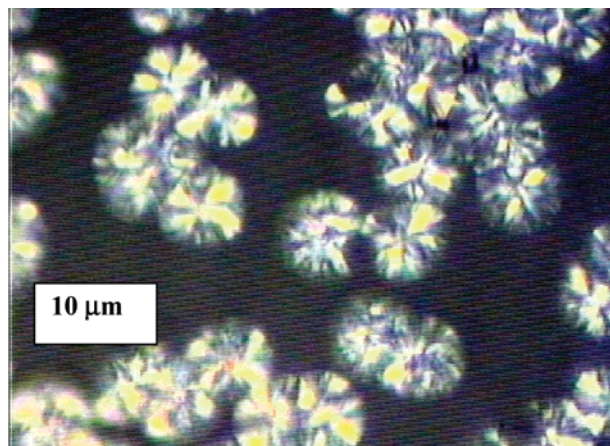


Figure 6. Polarized light micrograph of a PC-ZnSPS10.0 (80/20) blend annealed at 190 °C for 16 h.

Avrami equation to the crystallization kinetics in Figure 3 treating t_0 , K , and n as adjustable parameters.

The Avrami index depends on both the nucleation and growth of the crystal,³¹ so interpretation of the Avrami index requires an understanding of the crystal morphology. Figure 5 shows the WAXD pattern for PC-ZnSPS 10.0 before and after crystallization. Before annealing at 190 °C, the pattern showed only a diffuse amorphous peak for amorphous PC. After annealing the blend for 6 h at 190 °C, a peak at $q = 12.4 \text{ nm}^{-1}$ became apparent, and that peak became stronger and sharper as the crystallization progressed. The $q = 12.4 \text{ nm}^{-1}$ reflection corresponds to a Bragg spacing of $d = 0.505 \text{ nm}$, which is consistent with the spacing of the 020 and 201 planes of the orthorhombic unit cell of PC reported by Prietzsch,³² with $a = 1.19 \text{ nm}$, $b = 1.01 \text{ nm}$, and $c = 2.15 \text{ nm}$. The WAXD pattern of the crystallized PC-ZnSPS10.0 blend showed another weak reflection at $q = 17.9 \text{ nm}^{-1}$, which is related to the spacing of the -222 and 303 planes.³³ These data confirm that the PC crystals developed in the PC/ZnSPS (PC-ZnSPS) blend have the same structure as that reported for solvent and melt crystallized PC.¹ Figure 6 is a polarized optical micrograph of the spherulitic structure of a PC-ZnSPS10.0 blend crystallized for 16 h at 190 °C. The spherulites had a diameter of ca. $10 \mu\text{m}$. A similar spherulitic morphology was also observed for the PC-ZnSPS7.4 and PC-ZnSPS11.3 blends.

Table 2 summarizes the crystallization kinetic parameters obtained from the Avrami analysis. The Avrami index was essentially the same, ~ 3.0 , for all three blends. That corresponds to predetermined nucle-

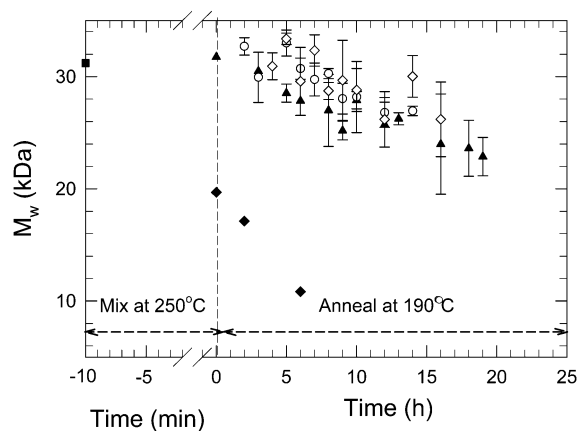


Figure 7. Effect of 250 °C preheat and 190 °C annealing on the weight-average molecular weight (M_w) of PC for PC-ZnSPS $x.y$ (80/20) blends ($x.y = 11.3$ (▲), 10.0 (●), 7.4 (◇)) and PC + 1% sodium benzoate, SB (◆). M_w of the PC prior the heat treatment is denoted by (■). The PC-ZnSPS $x.y$ (80/20) blends were first annealed at 250 °C for 10 min before annealing at 190 °C. PC and 1% SB were mixed at 250 °C for 7 min before annealing at 190 °C.

Table 2. Avrami Parameters for the Isothermal Crystallization of PC/ZnSPS Blends at 190 °C

blend	n	$K (\text{min}^{-n})$	$t_0 (\text{min})$
PC-ZnSPS7.4 (80/20)	2.9 ± 0.6	2×10^{-8}	110 ± 60
PC-ZnSPS10.0 (80/20)	3.3 ± 0.6	5×10^{-9}	40 ± 40
PC-ZnSPS11.3 (80/20)	2.9 ± 0.4	1×10^{-8}	370 ± 50

ation.³⁰ The induction times for the Avrami fits were ca. 2, 1, and 6 h for PC-ZnSPS7.4, PC-ZnSPS10.0, and PC-ZnSPS11.3, respectively. These are significantly shorter than that for pure PC, which is $>40 \text{ h}$ at 190 °C.^{2,23} As discussed above, the miscible blend, PC-ZnSPS11.3, exhibited a longer induction time than the two-phase blends. Two possible causes for the melt crystallization behavior of the PC-ZnSPS blends come to mind: (1) the ionomer nucleates crystallization or (2) the ionomer induces significant degradation of the PC, like the chemical nucleation results of Legras and co-workers,⁷⁻¹³ which lowers the melt viscosity sufficiently so that crystallization is more facile.

Effect of ZnSPS on the PC Molecular Weight.

The crystallization of PC in the PC-ZnSPS blend requires hours of annealing at relatively high temperature. Although pure PC is relatively stable at this temperature, the thermal stability of PC can be significantly influenced by the presence of a second component—as was discussed earlier in this paper for blends of PC with alkali metal salts of aryl carboxylates.⁷⁻¹³ Degradation of PC lowers the molecular weight, which also accelerates melt crystallization. Therefore, with regard to the SPS induction of PC crystallinity, it is important to ascertain whether PC degradation is the origin of that phenomenon.

Figure 7 shows how the weight-average molecular weight (M_w) of the PC component in the blend changed with increasing annealing time at 190 °C in the DSC for the blends prepared with the ionomers with the three highest sulfonation levels. The polydispersity of the PC remained nearly constant at ca. 1.8–2.1 for all blends. The molecular weight change for the PC in the blends during the 10 min preheat at 250 °C prior to annealing at 190 °C was $<5\%$. The PC molecular weight exhibited a slow decrease with increasing annealing time at 190 °C, and the decline of M_w was $\sim 25\%$ after

19 h. Pure PC did not exhibit a significant molecular weight change for a similar thermal history.

The amount of PC degradation appeared to increase with increasing sulfonation level. This contrasts with the observation described above that the rate of crystallization was faster for the blends with the two lower sulfonated ionomers, i.e., the PC–ZnSPS7.4 and PC–ZnSPS10.0 blends. In fact, neither of those blends exhibited significant PC degradation during the initial 4 h at 190 °C, during which time the PC crystallization started. That result suggests that the degradation was not responsible for the shorter crystallization induction times for the blends. If a molecular weight change was the key factor in determining the enhanced crystallization kinetics, one expects that the PC–ZnSPS11.3 would have crystallized faster than PC–ZnSPS7.4 and PC–ZnSPS10.0 instead of slower.

The effect of sodium benzoate (SB), on the degradation of PC is also shown in Figure 7; a substantial molecular weight decrease, ~30%, occurred during a 7 min preheat at 250 °C, and the degradation during annealing at 190 °C was also significant. These data are consistent with the results reported by Legras and co-workers^{7–13} in which the M_w of PC decreased by more than 40% after mixing PC and 1% SOCB for only 2 min at 270 °C. After annealing the PC/SB mixture for 5–6 h at 190 °C, part of the sample was no longer soluble, indicating that the PC cross-linked, which is also consistent with the effect of SOCB on PC reported by the Legras group. In contrast, no cross-linking of the PC was observed with the PC–ZnSPS blends either during the 250 °C preheat or the 190 °C annealing.

Although alkali metal salts of aromatic carboxylic acids, such as SOCB and SB, induced rapid melt crystallization of PC, once the polymer was melted at elevated temperature, the crystallization process was not repeatable.^{7–13} That result is in stark contrast to the crystallization/melting behavior of the PC–ZnSPS blends where the PC could be repeatedly crystallized and melted, which supports the conclusion that the crystallization of the PC in the PC–ZnSPS blends was not due to the same “chemical nucleation” mechanism as described by Legras and co-workers^{7–13} for the PC/arylcarboxylate salt mixtures.

For the PC/ionomer system the decrease in molecular weight during annealing at 190 °C may be due to reaction of the zinc sulfonate groups and water with the PC and/or degradation of the PC by the products of desulfonation of the ionomer. The degradation mechanism will be discussed in more detail in a separate paper. The important point, however, for the current paper is that degradation of the PC, by itself, does not provide a credible explanation for the enhanced crystallization behavior of the PC blended with the ZnSPS ionomer. One might also expect that the amount of degradation that did occur would not adversely affect the mechanical properties of the PC as does the addition of SOCB, though no mechanical data are yet available to support that hypothesis.

Model Mixture Studies. The results discussed in the previous section led to the conclusion that PC degradation is not alone responsible for the melt crystallization of the PC in the PC/ionomer blends. Since PS neither accelerates the crystallization of PC nor promotes its degradation, it is logical that the zinc sulfonate groups must in some way be responsible for the melt crystallization. To further investigate the origin

of the crystallization, the thermal behavior of model blends of PC and low molecular weight sulfonate salts, zinc, and sodium tosylate (ZnTS and NaTS) was investigated. Those mixtures are analogous to the PC/SOCB and PC/SOCP mixtures studied by Legras and co-workers,^{7–13} except for the difference in the base acid, i.e., sulfonic vs carboxylic. In this paper, only the thermal behavior of the model systems is discussed; more details on the chemistry of those systems and reactions of the tosylates with PC will be discussed in another paper.

The PC molecular weight in the PC–NaTS (98/2) and PC–ZnTS (99/1) mixtures did not change during the 10 min mixing at 250 °C in the Brabender mixer. That contrasts with the ~30% degradation of the M_w that occurred when SB was mixed at 250 °C with PC and the ~50% reduction in M_w when SOCB was mixed at 270 °C with PC for ca. 10 min.⁷ No PC crystallization was observed by DSC when the PC/tosylate mixtures were cooled after mixing or after annealing at 190 °C for 16 h. Relatively little change in the PC molecular weight occurred during the annealing process; the change in M_w of the PC–NaTS (98/2) was not significant, and the change for the PC–ZnTS (99/1) was <5%.

The thermal stability and the crystallization behavior of PC in the presence of the tosylate salts and the arylcarboxylate salts^{7–13} were much different. The arylcarboxylate is a strong nucleophile that can attack the carbonyl carbon of PC and cause fast interchange reactions, especially in a basic environment. The tosylate group, however, is a much weaker nucleophile that should be less effective at attacking the carbonyl carbon group or promoting interchange reactions within the PC chain. That also accounts for the much smaller effect of the ZnSPS on the PC molecular weight than that produced by the aryl carboxylate salts.

The difference between the crystallization behavior of the PC mixtures with the ionomer and with the tosylates is less clear. This may be due in part to the larger molecular weight change of the PC in the presence of the ionomer, or it may be due to differences in the dispersion and morphology of the sulfonate groups in the two compounds. The molecular weight difference seems a less likely explanation for two reasons. First, the molecular weight changes in the polymer blends (see discussion above) were actually small and comparable to those for the ZnTS blend when crystallization began. And, second, the molecular weight of the PC in the polymer blends after 19 h of annealing were still comparable to many grades of PC, which do not exhibit melt crystallization.

Differences in the dispersion of the salt groups seem to be a more plausible explanation for the differences in crystallization between the ionomer and tosylate mixtures. The PC/ionomer blends were partially miscible, and the particular blends studied were either single phase or phase-separated with a PC-rich dispersed phase that contained some dissolved ionomer. In contrast, the PC/tosylate mixture was grossly phase-separated, with particle sizes as large as 100 μm . The presence of a dispersed phase alone is insufficient for nucleating melt crystallization of PC, as evident the results from PC/PS blends and from the PC/tosylate blends. Furthermore, the melt crystallization of the PC–ZnSPS11.3 blend, which was single phase, indicates that a second macrophase is not necessary for the PC crystallization. By elimination, this points to the zinc

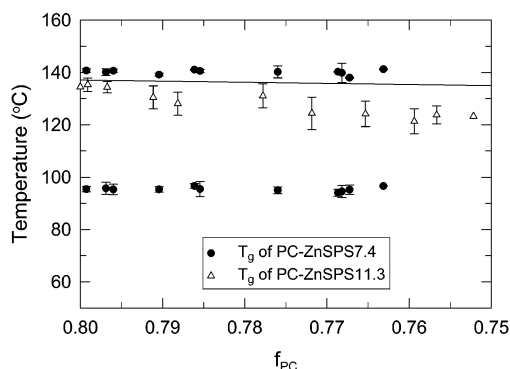


Figure 8. T_g 's determined by DSC for PC–ZnSPS7.4 (80/20) blend and PC–ZnSPS11.3 (80/20) blends as a function of composition of PC in the amorphous phase. The composition of PC in the amorphous phase was calculated from eq 2. The solid line represent the Fox equation³⁴ prediction of T_g for the PC–ZnSPS11.3 (80/20) blend.

sulfonate groups as being responsible for the PC nucleation. Again, two different mechanisms come to mind. First, that the ionic nanodomains that are found in the neat ionomer persist in the PC–ZnSPS blends and act as nucleation sites. Or, second, a specific chemical interaction or reaction between the PC and the zinc sulfonate promotes nucleation. In that case, the excellent dispersion of the ionomer, and therefore the sulfonate groups in the PC, as opposed to the poor mixing of the tosylate in PC, could play an important role. Still, the crystallization induction times for the phase-separated PC/ionomer were shorter blends than for the miscible blend, which suggests that the nucleation is more complicated than a simple mechanism involving the zinc sulfonate groups. That is, the second phase also would seem to play a role, but that a fine dispersion of zinc sulfonate groups is required. Unfortunately, none of the experiments performed thus far have unambiguously identified the exact mechanism of nucleation, so that that question remains unresolved. Discussion of possible sources of the crystal nucleation will be discussed later in this paper.

Phase Behavior during Crystallization. The crystallization of a polymer blend may be complicated by the possibility of simultaneous phase separation. Coupling of the two processes may perturb the crystallization kinetics and/or produce unusual microstructures.

If one assumes that the ZnSPS resides only in the amorphous phase, which is a reasonable assumption, one can calculate the concentration (mass fraction) of PC in the amorphous phase during the crystallization is given by the following equation

$$f_{PCa} = \left(0.8 - \frac{\Delta H_f}{\Delta H_f} \right) \left[\left(0.8 - \frac{\Delta H_f}{\Delta H_f} \right) + 0.2 \right] \quad (5)$$

where ΔH_f is the enthalpy of fusion calculated from the DSC endotherm and ΔH_f is the heat of fusion for 100% crystalline PC.

The T_g (s) measured by DSC for the PC–ZnSPS7.4 and PC–ZnSPS11.3 blends that were isothermally crystallized at 190 °C (see Figure 5) are plotted against the mass fraction of PC in the amorphous phase, as calculated from eq 2, in Figure 8. PC–ZnSPS7.4 was a partially miscible blend (see the miscibility diagram shown in Figure 2). As the PC crystallized, the total concentration of PC in the amorphous phase decreased,

and according to Figure 2, the amorphous phase should remain phase-separated. The blend exhibited UCST liquid–liquid phase behavior,^{14,15} and at constant temperature, i.e., the 190 °C crystallization temperature, the compositions of the two amorphous phases should remain constant as the amount of PC in the amorphous phase decreased; i.e., only the amount of each phase should change. This is supported by the detection of two invariant T_g 's, one corresponding to a mixed PC/ionomer phase and the other a pure ionomer phase, for all the samples of PC–ZnSPS7.4.

PC–ZnSPS11.3 was miscible at 190 °C prior to crystallization. According to the miscibility diagram shown in Figure 2, decreasing the PC concentration of the amorphous phase moves that phase closer to the boundary for the single- and two-phase regions. Although the diagram shown in Figure 2 indicates that the amorphous phase should remain single phase up to at least a 40 wt % concentration of the ionomer, the T_g data shown in Figure 8 for the crystallized blends suggest that this may not have been the case. Although only a single T_g was detected, the T_g decreased much more rapidly with increasing crystallization than would be expected if the only effect were the dilution of the PC content. The Fox equation,³⁴ a commonly used equation for predicting the T_g of a miscible blend, prediction is plotted in Figure 8, and it substantially overestimated the measured T_g . One possible explanation for the lower T_g is the lowering of the molecular weight during the crystallization process, but a change in M_w from 30 to 20 kDa should only account for about a 4 °C decrease in T_g , which is smaller than that observed. The other possibility is that some phase separation may have occurred during the crystallization process. One should note that the uncertainty of the “phase boundary” drawn in Figure 2 may be quite large, since its construction depends on the detection of a two T_g 's, which is problematic near the phase boundary when the amount of one of the phases is small.

FT-IR Analysis of Chemical Interactions. In the case of miscible and partially miscible blend, specific interactions between the two polymers in the blend are often observed. Weiss and co-workers^{14–16} previously reported that FTIR analysis failed to detect any specific interactions between PC and the ionomer in miscible blends of PC–NaSPS and PC–ZnSPS. They attributed the miscibility in those systems to the strong “repulsive” interactions within the ionomer. In the current paper, the FTIR investigation of the PC/SPS system was extended to include samples that were annealed for extended time at 190 °C. The motivation for these new studies was to assess whether the FTIR spectra changed as a result of crystallization and/or degradation of the PC in the blend. These studies concentrated on the PC–ZnSPS11.3 blend, which exhibited the largest molecular weight change during the crystallization.

Figure 9a shows the FTIR spectra of the sulfonate stretching region of the component polymers and the PC–ZnSPS11.3 after annealing at 190 °C for various times. The absorption band at 1039 cm^{-1} , which is due to the symmetric stretching vibration of the SO_3^- anion with a Zn^{2+} cation, is very sensitive to the local chemical environment change. Any weakening of the ion-pair interaction, such as would occur if the Zn^{2+} or the SO_3^- were involved with a specific interaction with PC, should shift that absorption. Figure 9a shows that neither the position nor the shape of the peak at 1039 cm^{-1} changed

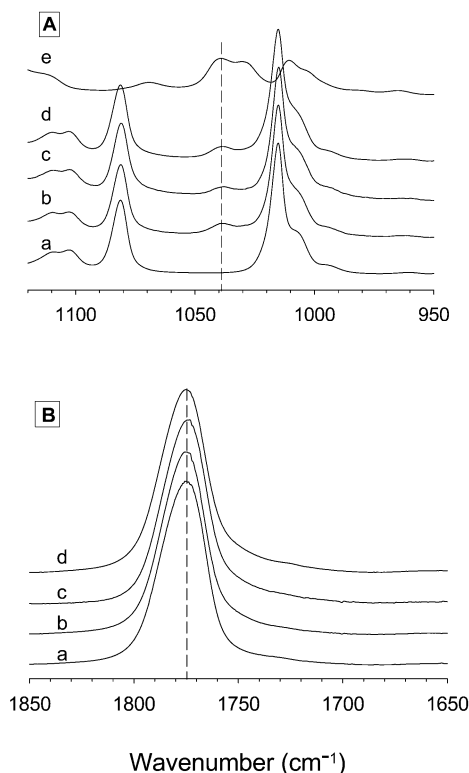


Figure 9. FTIR spectra of (A) the sulfonate stretching region and (B) the carbonyl stretching region for (a) neat PC; PC-ZnSPS11.3 (80/20) blends annealed at 190 °C for (b) 8 h, (c) 12 h, and (d) 18 h; and neat ZnSPS11.3 (e).

during the thermal annealing at 190 °C, and the peak was essentially identical with that in the neat ionomer.

Figure 9b shows the FTIR spectra of the carbonyl stretching region for the same samples used to construct Figure 9a. The absorption band at 1775 cm⁻¹ is due to the stretching vibration of the carbonyl groups in PC, and this band should also be sensitive to any interactions with the ionomer. The carbonyl group is the most likely site of a specific ionomer-PC interaction. The position and shape of the absorption at 1775 cm⁻¹ showed no discernible change upon addition of ZnSPS to PC or during annealing at 190 °C. The FTIR spectra shown in Figure 9 do not indicate any specific interaction between the sulfonate and carbonate group, though it is still possible that the interaction responsible for crystallization is either very dilute or transient and not sufficiently long-lived to detect after cooling the sample.

Ionomer Microstructure in Blends. The microstructure of neat SPS ionomers consists of microphase-separated ion-rich domains dispersed within an ion-poor continuous phase,³⁵ and the microphase-separation persists to temperatures > 250 °C.³⁶ Evidence for the microphase separation is provided by a peak in the SAXS pattern, as shown in Figure 10 for the ZnSPS11.3 sample at 190 °C. The broad peak in the scattering structure factor is centered about $q = 1.9 \text{ nm}^{-1}$, which corresponds to a correlation size of 3.3 nm in real space. The ionomer SAXS peak was also observed in the PC/ionomer blends, as seen for the PC-ZnSPS11.3 blend at 190 °C shown in Figure 10. Earlier in this paper, on the basis of thermal analysis and sample clarity, it was concluded that the PC-ZnSPS11.3 was single-phased, which indicates that although miscible with the PC, the microphase-separated microstructure of the ionomer was retained in the blend. That result is not completely

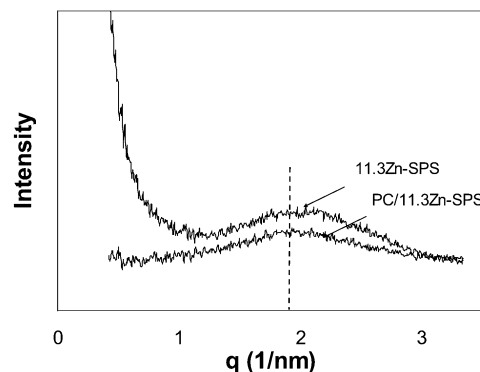


Figure 10. SAXS intensity as a function of scattering vector (q) for neat ZnSPS11.3 and the PC-ZnSPS11.3 (80/20) blend. The dashed line corresponds to $q = 1.9 \text{ nm}^{-1}$.

surprising in that there were no discernible specific chemical interactions between the two polymers, which might have been expected to solvate the ion-dipole associations within the ionomer.

Prior to crystallization, the morphology of the “miscible” PC/ionomer blends consisted of nanometer-sized ionic domains dispersed within a single-phase mixture of PC and essentially PS. In contrast, the two-phase PC/ionomer blends exhibited a morphology of micrometer-sized domains of the ionomer, which was composed of nanometer-sized ionic domains within essentially a PS continuous phase, dispersed within a continuous mixed phase of PC and some ionomer. Furthermore, the SAXS results of the miscible PC-ZnSPS11.3 blend also suggest that the PC-rich phase for the two-phase blends also contained nanometer-sized ionic domains, though from the SAXS data, there is no way to assign the ionic domains to either or both of the macrophases.

Figure 10 does show some differences between the SAXS of ZnSPS11.3 and PC-ZnSPS11.3 for $q < 0.9 \text{ nm}^{-1}$, which correspond to sizes of >7 nm. The neat ionomer exhibited a large upturn in intensity at low q , while the blend did not show any significant intensity increase for q as low as 0.4 nm^{-1} , which corresponds to about 15 nm. The intensity increase at low q for ionomers is believed to result from a heterogeneous distribution of nonaggregated ionic groups.³⁷ Thus, the difference in the low- q region of the SAXS curves for the ionomer and the blend in Figure 10 may indicate a change in the spatial distribution of nonaggregated ionic species, though unfortunately, as with ionomers in general, the details of those distributions are not determinable from the SAXS data.

Melt Nucleation of PC Crystallization. The PC-ZnSPS blends used in this study included both single-phase and two-phase morphologies. As discussed in the preceding section, in both types of samples, microphase-separated ionic domains formed from the ionomer component. Also, as discussed earlier in this paper, melt crystallization of PC occurred in both types of morphologies, and the induction time for crystallization depended on the sulfonation level of the ionomer. In general, increasing the sulfonate content of the ionomer decreased the crystallization induction time, though the morphology of the blend also influenced the crystallization kinetics. Although the rates of the crystallization were similar in the two morphologies, i.e., single and two phase, for similar sulfonation levels, the crystallization induction time was significantly shorter for the two-phase blend.

The Avrami analysis indicated that the PC crystallization was nucleated. The induction time is related to the nucleation process. For a pure polymer melt, the nucleation step involves the folding of polymer chains and the formation of solid surfaces that become the nuclei for crystallization; the energy barrier for this process is usually very high.³⁸ The preexistence of a foreign solid surface in the melt can accelerate the nucleation step.³⁸ One might presume that phase-separated ionomer domains may represent nucleation sites, but two facts discount that explanation. First, PC/PS blends are also phase-separated and the PS domains did not induce PC crystallization. Second, melt crystallization of PC also occurred in the single-phase PC/ionomer blends, so clearly a micrometer-size domain is not solely responsible for nucleating the PC crystallization. That leaves the sulfonate groups as the most logical origin of the nuclei, and here there are two potential sources: (1) isolated sulfonate groups, or more likely, small multiplets of associated sulfonate groups and (2) the larger nanometer-sized ionic aggregates. Unfortunately, the data obtained in this study cannot distinguish the role of these two possibilities or whether both types of species play a part in the crystallization process.

A couple of observations merit additional comment, though unfortunately, they add questions rather than answers to the puzzle of the origin of nucleation. The FTIR study indicated that there was no specific interaction between the Zn sulfonate groups and the PC. That suggests that it is the nanometer-sized ionic domains rather than individual sulfonate groups that are the nucleation sites. Yet, that hypothesis does not explain why the two-phase blend was more effective at nucleating the PC crystallization. Perhaps, in the macrophase-separated blend, the ionic groups or ionic domains tend to aggregate at the ionomer-PC interface, but no evidence for that was obtained in the present study.

Conclusions

The addition of ZnSPS ionomers to bisphenol A polycarbonate accelerates the melt crystallization of PC. An Avrami analysis indicated that the crystallization was a nucleated process. Melt crystallization of PC was observed in both single-phase (i.e., miscible) and phase-separated blends. The sulfonate groups, either as individual species (or multiplets) or as nanometer-sized ionic aggregates, are the most likely origin of the nucleation, but the specific details of the process were not determined. Evidence of the ionic aggregates, as are usually observed in neat ionomers, was obtained for both the single-phase and phase-separated blends. But, while the sulfonate groups or ionic domains were prime suspects for the origin of the nucleation, the fact that the crystallization induction time was faster for phase-separated blends indicates that the presence of a macrophase, i.e., a micrometer-size phase of pure SPS, also contributed and actually accelerated the nucleation of crystallites. Attempts to further uncover the precise origin and mechanism of the nucleation, however, were not successful.

Melt nucleation of PC by the addition of organic carboxylate salts has been previously reported.⁷⁻¹³ Although the observation of melt crystallization of PC by the sulfonated ionomers described herein and by the arylcarboxylate salts in refs 7-13 are similar, the mechanisms are completely different. The crystalliza-

tion induced by the carboxylate salts, termed "chemical nucleation" by those authors, is an irreversible process that also severely degrades the PC. The addition of ZnSPS ionomers to PC does reduce the molecular weight if the blend is aged in the melt for very long times, but the extent of degradation is significantly less than what occurs with the organic carboxylate salts and the crystallization that results is completely reversible. That is, the material can be repeatedly melted and recrystallized.

Crystallization is expected to impart improved solvent resistance to PC, which provides a potential application of the blends described herein. But, while the crystallization rates for the PC-ZnSPS blends may be orders of magnitude faster than for neat PC, the crystallization process is still slow, of the order of 10 h at 190 °C to achieve >20% crystallinity. A future topic for study is whether stress, such as would naturally occur in typical polymer melt processing operations, can further accelerate crystallization, so that reasonable crystallization times may be achieved. Stress-induced crystallization is a well-known phenomenon, and order of magnitude decreases in crystallization time of thermoplastics can be achieved by applying stress during crystallization.

A limitation of this investigation was that it only considered one blend composition, 80/20 (w/w) PC/ionomer. If ZnSPS were to be used as an additive to PC, one might reasonably expect that relatively low concentrations would be most desirable. However, at sufficiently high sulfonation levels, e.g., 11.3 mol %, the ionomer is miscible with PC, and as a consequence, one may obtain a smaller compromise of the properties of the PC with relatively high amounts of the ionomer than for a phase-separated material where the glassy ionomer domains would embrittle the PC. Still, in the absence of mechanical property data, which were not obtained in this study, we hesitate to speculate further on the compositions that would be commercially practical—if any. A mechanical property study is another topic for future consideration, but larger quantities of ionomer samples are needed than were possible in this study.

Acknowledgment. This work was supported by a grant from the Polymer Program of the National Science Foundation (DMR 9712194).

References and Notes

- (1) Garbaskas, M. F. In *Handbook of Polycarbonate Science and Technology*; LeGrand, D. G., Bendler, J. T., Eds.; Marcel Dekker: New York, 2000; p 293.
- (2) Turska, E.; Przygocki, W.; Maslowski, M. *J. Polym. Sci., Part C* **1968**, *16*, 3373-3377.
- (3) Mercier, J. P.; Groeninckx, G.; Lesns, M. *J. Polym. Sci., Part C* **1967**, *16*, 2059-2067.
- (4) Heiss, H. L. *Polym. Eng. Sci.* **1979**, *19*, 625-637.
- (5) Beckman, E.; Porter, R. S. *J. Polym. Sci., Part B: Polym. Phys.* **1987**, *25*, 1511-1517.
- (6) Gallez, F.; Legras, R.; Mercier, J. P. *J. Polym. Sci., Part B: Polym. Phys.* **1976**, *14*, 1367-1377.
- (7) Legras, R.; Bailly, C.; Daumerie, M.; Dekoninck, J. M.; Mercier, J. P. *Polymer* **1984**, *25*, 835-844.
- (8) Bailly, C.; Daumerie, M.; Legras, R.; Mercier, J. P. *J. Polym. Sci., Polym. Phys. Ed.* **1985**, *23*, 343-354.
- (9) Bailly, C.; Daumerie, M.; Legras, R.; Mercier, J. P. *J. Polym. Sci., Polym. Phys. Ed.* **1985**, *23*, 355-366.
- (10) Bailly, C.; Daumerie, M.; Legras, R.; Mercier, J. P. *J. Polym. Sci., Polym. Phys. Ed.* **1985**, *23*, 493-507.
- (11) Bailly, C.; Daumerie, M.; Legras, R.; Mercier, J. P. *J. Polym. Sci., Polym. Phys. Ed.* **1985**, *23*, 751-770.

- (12) Bailly, C.; Daumerie, M.; Legras, R.; Mercier, J. P. *Makromol. Chem.* **1986**, *187*, 1197–1214.
- (13) Bailly, C.; Legras, R.; Mercier, J. P. *Polym. Prepr. (Am. Chem. Soc., Div. Polym. Chem.)* **1985**, *26* (2), 170–171.
- (14) Xie, R.; Weiss, R. A. *Polymer* **1998**, *39*, 2851–2858.
- (15) Xie, R.; Weiss, R. A. *Mater. Res. Soc. Symp. Proc.* **1997**, *461*, 13–18.
- (16) Lu, X.; Weiss, R. A. *Macromolecules* **1996**, *29*, 1216–1221.
- (17) Xu, L.; Weiss, R. A. *Polym. Prepr. (Am. Chem. Soc., Div. Polym. Chem.)* **2000**, *41* (2), 1155–1156.
- (18) Makowski, H. S.; Lundberg, R. D.; Singhal, G. H. U.S. Pat. 3,870,841, 1975.
- (19) Kambour, R. P.; Bendler, J. T.; Bopp, R. C. *Macromolecules* **1983**, *16*, 753–757.
- (20) Paul, D. R.; Barlow, J. W. *Polymer* **1984**, *25*, 487–494.
- (21) Ten Brinke, G.; Karasz, F. E.; Macknight, W. J. *Macromolecules* **1983**, *16*, 1827–1832.
- (22) Peilstöcker, G. *Kunststoffe* **1961**, *59*, 509–515.
- (23) Alizadeh, A.; Sohn, S.; Quinn, J.; Marand, H.; Shank, L. C.; Iler, H. D. *Macromolecules* **2001**, *34*, 4066–4078.
- (24) Sohn, S.; Alizadeh, A.; Marand, H. *Polymer* **2000**, *41*, 8879–8886.
- (25) Jonza, J. M.; Porter, R. S. *J. Polym. Sci., Polym. Phys.* **1986**, *24*, 2459–2472.
- (26) Mercier, J. P.; Legras, R. *J. Polym. Sci., Polym. Lett.* **1970**, *8*, 645–650.
- (27) Hoffman, J. D.; Weeks, J. J. *J. Chem. Phys.* **1965**, *42*, 4301–4302.
- (28) Christopher, W. F.; Fox, D. W. *Polycarbonate*; Reinhold: New York, 1962; p 24.
- (29) Legras, R.; Mercier, J. P. *J. Polym. Sci., Polym. Phys.* **1977**, *15*, 1283–1289.
- (30) Avrami, M. *J. Chem. Phys.* **1941**, *9*, 177–184.
- (31) Hay, J. N. *Br. Polym. J.* **1971**, *3*, 74–82.
- (32) Prietzschk, V. A. *Kolloid Zh.* **1958**, *156*, 8–14.
- (33) Fryer, R. E. J. *J. Appl. Polym. Sci.* **1974**, *18*, 2261–2268.
- (34) Fox, T. G. *Bull. Am. Phys. Soc.* **1956**, *1*, 123.
- (35) Peiffer, D. G.; Weiss, R. A.; Lundberg, R. D. *J. Polym. Sci., Polym. Phys. Ed.* **1982**, *20*, 1503–1509.
- (36) Weiss, R. A.; Lefelar, J. A. *Polymer* **1986**, *27*, 3–10.
- (37) Register, R. A.; Ding, Y. S.; Foucart, M.; Jerome, R.; Hubbard, S. R.; Hodgson, K. O.; Cooper, S. L. In *Multiphase Polymers: Blends and Ionomers*; Utracki, L. A., Weiss, R. A., Eds.; *Adv. Chem. Ser.* **1989**, *395*, 420.
- (38) Wunderlich, B. *Macromolecular Physics*; Academic Press: New York, 1973; Vol. 1.

MA035057V